

Estimation of snow water equivalent from MODIS Albedo for a non-instrumented watershed in Eastern Himalayan Region

Grace Nengzouzam¹, Ngahorza Chiphang¹, Shelina Rajkumari¹, Liza G Kiba¹, Arnab Bandyopadhyay^{2*}, Aditi Bhadra²

¹Research Scholar, Department of Agricultural Engineering, North Eastern Regional Institute of Science and Technology, Nirjuli (Itanagar), Arunachal Pradesh 791109, India.

²Associate Professor, Department of Agricultural Engineering, North Eastern Regional Institute of Science and Technology, Nirjuli (Itanagar), Arunachal Pradesh 791109, India.

*Corresponding authors email: arnabbandyo@yahoo.co.in

Submitted: 30/4/2018 Accepted: 12/3/2019 Published online: 29/3/2019

Abstract

Snow water equivalent (SWE) quantifies the amount of water present in a snowpack. Water in a snowpack is dependent on its depth, density, type of snow, previous freezing-thawing cycles, recent precipitation events, etc. This study deals with estimation of snow depth (HS) and snow density (RHO) from remotely sensed data using empirical relationships developed elsewhere and thereby generation of SWE maps and assessing the usability of such approach for non-instrumented eastern Himalayan watersheds. Remotely sensed data: digital elevation model (DEM), MODIS (Moderate Resolution Imaging Spectroradiometer) land surface temperature (LST), snow albedo, fractional snow cover and precipitation were used as inputs. Models were developed to find out the RHO, HS and SWE at pixel level. Finally, the SWE maps were generated for the dominating snow months of the year 2013. Results showed that RHO increased from January to May with its peak in the month of May having considerable amount of ripened snow. HS and SWE were found to follow the same trend as SCA (Snow Covered Area), which increased from January to peak in February and then decreased till May. The estimated RHO, HS and SWE were found acceptable in comparison to other published data collected from relevant research works on the Himalayan region and SWE from Global Land Data Assimilation Systems NOAA Land Surface Model (GLDAS NOAA LSM) simulation.

Keywords: MODIS BRDF/Albedo, Snow water equivalent, Snow depth, Snow density, Snow covered area, Himalaya.

1. Introduction

The Himalayan region, often referred as the third pole of the earth, comprises of huge snow covered areas and is a major fresh water reserve. Snowmelt releases large amount of fresh water in the rivers and its accurate estimation is important for water managers. In mountainous catchments, snowmelt typically constitutes a significant part of the total runoff (Takala et al., 2011). If the snowpack melts, amount of water that would be released depends on the snow water equivalent (SWE) of the snowpack and the vertical height of the snowpack on the ground is the snow depth. Although, the actual amount of water flowing through the river would depend on many other factors such as evapotranspiration and infiltration, but quantifying the water stored in a snowpack is important first-hand information. The spatial and temporal distribution of SWE is

also important for managing mountain water resources and its future predictions. Also, to make sound water management decisions, it is essential that the SWE of the snowpack is accurately estimated. For hydrological applications, the snow cover must be characterized by its SWE, which is strongly correlated to the depth of the snowpack (Elder et al., 1998; Hassan et al., 2012). This correlation could potentially be used to estimate SWE from snow depth, as measuring SWE directly requires substantial efforts.

Remote sensing techniques make it easier to estimate snow-water content from measured albedo in inaccessible mountain areas. The relation between snowpack density and albedo has been investigated by some researchers. Smith and Halverson (1979) developed a method for estimating average snowpack density by measuring solar albedo based on an

empirical relationship between average snowpack density and the snow surface albedo. A relationship between the snowpack density and snow depth with other independent physiographic variables like Julian day, UTM-easting, elevation has also been reported (Sexstone and Fassnacht, 2014). Researchers have also shown that SWE can be calculated from snow depth if the snow bulk density is known. Jonas et al. (2009) attempted to estimate the SWE from snow depth and developed regression equation to model snow density as a function of season, snow depth, site altitude, and site location. Bavera et al. (2007) showed that, the spatial distribution of SWE over a basin can be successfully estimated by merging field measurements of density with remotely sensed snow-covered area. On the other hand, Avanzi et al. (2015) cautioned to take due care in using such regression equations for estimating snow bulk density, especially in high elevation areas. Stigter et al. (2017) estimated SWE and snowmelt runoff in a Himalayan catchment using satellite snow cover data and ground measurements of snow depth and observed a strong gradient of increasing SWE with increasing elevation.

Due to harsh terrain and inaccessible mountainous region of Eastern Himalaya, it is difficult to have direct observations of snow density, snow depth and SWE on the ground and hence, use of satellite data render a more feasible approach. Although such studies have been done in European and American mountains, but, since most of the approaches are empirical in nature, they warrant specific validation in Himalayan, especially in Eastern Himalayan region. The current study was undertaken to study the possibility of determining snow density, snow depth and snow water equivalent maps for a non-instrumented watershed of Eastern Himalayan region with remotely sensed data and to check the accuracy of the estimated SWE against other published SWE product.

2. Materials and methods

2.1. Study area

This study was conducted in a small 52 km² seasonally snow covered catchment

named Nuranang (Fig. 1). It is situated in Tawang district of Arunachal Pradesh, India. The stream, a tributary to Tawang River, originates from Sela Lake and ends as Nuranang falls at Jang. The Central Water Commission (CWC) discharge site was selected as the outlet point of the catchment which lies at 27° 33' 01" N and 92° 01' 13" E, with an elevation of 3143 m above mean sea level (MSL). The catchment is situated between latitudes 27°30' and 27°35' N, and longitudes 92°00' and 92°07' E. Elevation of the basin ranges from 3,143 m to 4,946 m above MSL with an average slope of 51%. Monsoon season is from June to September with average annual precipitation of 1,139 mm. The catchment gets covered by seasonal snow during November to May. Snow starts accumulating from October and ends at May.

2.2. Data Acquisition

In this study MODIS (MOD10A1-V005) (Hall et al., 2006) daily snow cover product available at 500 m resolution was used. MOD10A1 is produced and distributed by the NASA Distributed Active Archive Centre (DAAC) situated at the National Snow and Ice Data Centre (NSIDC) (<http://reverb.echo.nasa.gov/reverb/>). MOD10A1 images on daily basis for the snow block year of 2012–2013 (October 2012–May 2013) were downloaded and the albedo and fractional snow cover layer of MOD10A1 were used to obtain the SWE and snow covered area (SCA) percentage, respectively. Shuttle Radar Topography Mission (SRTM) digital elevation model (DEM) with 90 m resolution was used for delineating the catchment area as well as for elevation data. MODIS Land Surface Temperature (LST day and LST night) data from its MOD11A1 product for the same period was used as a proxy to temperature data. The precipitation data for the snow block year of 2012–2013 (October 2012–May 2013) were obtained from Tropical Rainfall Measuring Mission (TRMM) (<http://sharaku.eorc.jaxa.jp/GSMaP/>) on hourly basis.

2.3. Pre-Processing of data

The downloaded MODIS albedo images were in compressed Hierarchical Data Format-

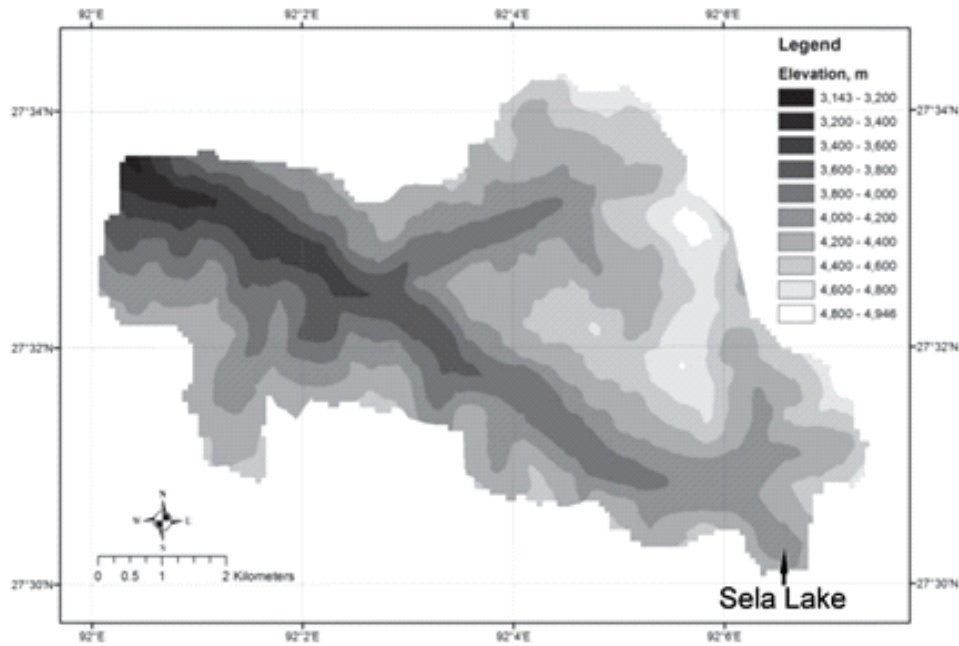


Fig. 1. Nuranang river catchment, Arunachal Pradesh, India.

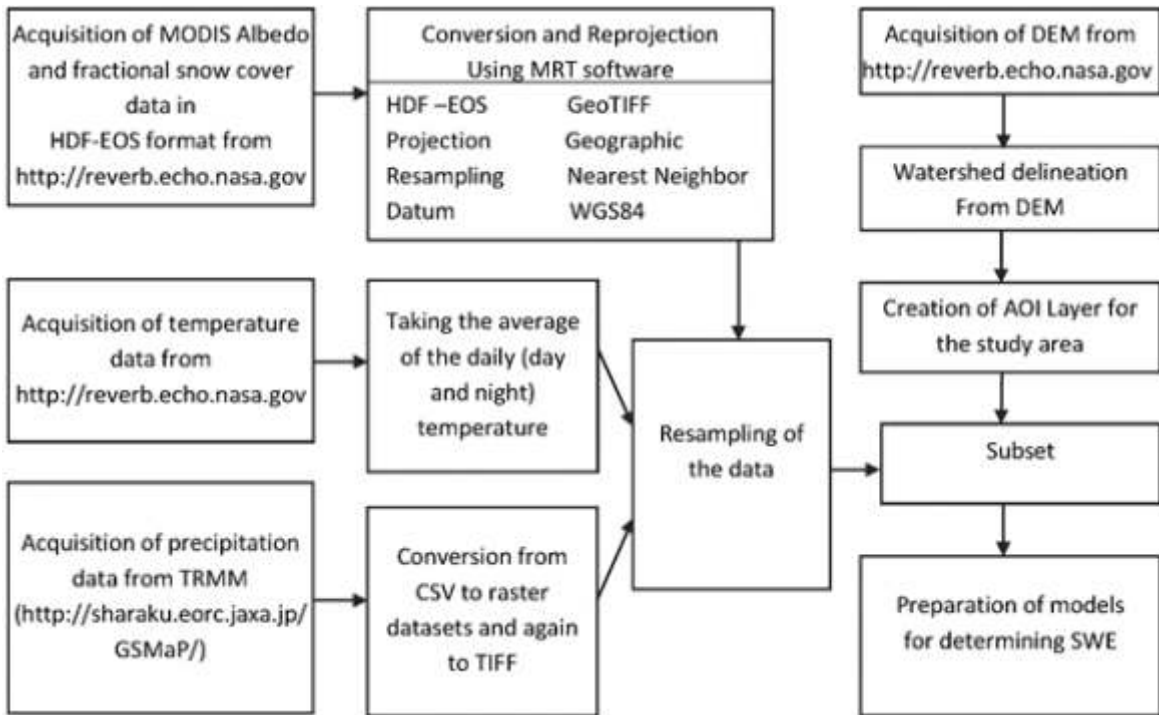


Fig. 2. Flowchart illustrating the data pre-processing steps.

Earth Observing System (HDF-EOS) format accompanied by corresponding metadata. To convert the HDF-EOS to GeoTIFF, MODIS Re-projection Tool (MRT) (version 4.1) was used. The MODIS Reprojection Tool was downloaded from https://lpdaac.usgs.gov/tools/modis_reprojection_tool. The downloaded HDF files were used as input to the MRT; the projection was set to Geographic with datum as World Geodetic System 84 (WGS84), resampling method was selected as Nearest Neighbour, and the files were converted from HDF-EOS to GeoTIFF format. As the albedo data were the base information used in this study for estimating snow density, leading to estimation of SWE, assessing the accuracy of the input albedo data was important. The MODIS records the shortwave albedo values for snow/ ice covered pixels that are cloud-free. However, the MOD10A1 daily albedo product may contain unsubstantiated errors in mountainous regions since it is a beta-test product (Chiphang et al., 2017). Therefore, hourly mean Albedo (both incoming and outgoing) data from October 2012 to May 2013 were collected from automated weather station (AWS) installed near Sela lake at an elevation of 4,211 m above MSL at 27° 30' 15" N and 92° 06' 16" E. To assess the accuracy of daily albedo values obtained from MODIS product for cloud-free dates were compared with the AWS measured daily albedo values. Although the accuracy of the same MODIS product (MOD10A1 and MYD10A1) for the same catchment has been assessed for another layer (fractional snow cover) (Mishra et al., 2016) and the broadband snow albedo derived from AWiFS data for this catchment matched quite well with the MODIS albedo after some bias correction (Bandyopadhyay et al., 2016), a pixel-by-pixel and day-by-day comparison between MODIS albedo and observed albedo could not be done due to very limited ground observations available during which the AWS pixel was cloud-free. In addition, the Science Quality flag (assigned by MODIS Land Science Team to evaluate the product samples) of MOD10A1 is set “Inferred Passed” which indicates the reliability of the data used.

The temperature data for day (LST day) and night (LST night) were resampled so as to get the same grid size for all input images and

converted to °C. A model was developed to find out the ratio of rainfall to total precipitation (rainfall + snowfall) in the last storm (R) based on mean temperature (Tmean) and critical temperature. The critical temperature for the region was taken as 2.5 °C (Senzeba et. al., 2015) and the daily Tmean was determined as the average of LST day and LST night. Then the value of R was determined as:

$R = 0$, if $T_{mean} < 0$ °C (indicates snowfall only)

$R = 1$, if $T_{mean} > 2.5$ °C (indicates rainfall only) and

$R = 0.5$, if $0 < T_{mean} < 2.5$ °C (indicates mixture of rain and snow in equal proportion)

The hourly precipitation data, which were in comma separated value (CSV) file format along with their corresponding metadata were pre-processed to bring it in TIFF format. All 24 hourly raster layers corresponding to a day were summed up to get the daily precipitation layers. Similar to temperature layers, the daily precipitation layers were also resampled to the same resolution.

The downloaded DEM was pre-processed for delineating the watershed with the Central Water Commission (CWC) discharge site considered as the outlet point. This watershed polygon was used as the AOI (Area of Interest) layer to clip the above mentioned data layers.

2.4. Determination of snow density from snow albedo

The snow density can be determined from snow albedo as given below (Smith and Halverson, 1979):

$$RHO = [0.452 - 0.123 A^2 + 0.003 SD_{degree} + 0.002 D + 0.027 R - 0.039 ZCOS + E] 1000 \quad (1)$$

where, RHO = snowpack density, kg m⁻³; A = albedo, fraction; D = days since cessation of storm, integer; R = proportion of rain to snow in last storm: 0, 0.5 or 1; ZCOS = cosine of the solar zenith angle; SD = solar declination, degrees; E = 0.037 g cm⁻³.

The solar declination (SD) and the ZCOS

can be determined using the equations for the general solar position calculations. First, the fractional year (γ , rad) is calculated as below:

$$\gamma = \frac{2\pi}{365} \left(\text{day of year} - 1 + \frac{\text{hour}-12}{24} \right) \quad (2)$$

From γ , the equatorial time (eqtime, min) and the solar declination (SD) can be estimated as:

$$\text{eqtime} = 229.18 (0.000075 + 0.001868 \cos \gamma - 0.032077 \sin \gamma - 0.014615 \cos 2\gamma - 0.040849 \sin 2\gamma) \quad (3)$$

$$\begin{aligned} SD_{\text{radian}} = & 0.006918 - 0.399912 \cos \gamma + 0.07025 \\ & \sin \gamma - 0.006758 \cos 2\gamma + 0.000907 \sin 2\gamma - \\ & 0.002697 \cos 3\gamma + 0.00148 \sin 3\gamma \quad (4) \end{aligned}$$

$$SD_{\text{degree}} = SD_{\text{radian}} \left(\frac{180}{\pi} \right) \quad (5)$$

Then, time offset (time offset, min) and true solar time (tst, min) are calculated as below:

$$\begin{aligned} \text{time offset} = & \text{eqtime} - (4 \text{ longitude}_{\text{degree}}) \\ & + (60 \text{ timezone}) \quad (6) \end{aligned}$$

$$\text{tst} = (60 \text{ hour}) + \text{minute} + \left(\frac{\text{second}}{60} \right) + \text{time offset} \quad (7)$$

Then the solar hour angle (HA) can be calculated as follows:

$$HA_{\text{degree}} = \left(\frac{\text{tst}}{4} \right) - 180 \quad (8)$$

$$HA_{\text{radian}} = HA_{\text{degree}} \left(\frac{\pi}{180} \right) \quad (9)$$

The cosine of the solar zenith angle (ZCOS) can then be found as below:

$$\begin{aligned} ZCOS = & \sin(\text{latitude}_{\text{radian}}) \sin(SD_{\text{radian}}) + \\ & \cos(\text{latitude}_{\text{radian}}) \cos(SD_{\text{radian}}) \cos(HA_{\text{radian}}) \quad (10) \end{aligned}$$

where, longitude degree = site longitude, degree; timezone = time difference with UTC (Coordinated Universal Time), h; hour = hour (0–23), minute = minute (0–59), second = second (0–59) corresponding to local time; latitude_radian = site latitude, rad.

2.5. Determination of SWE from snow depth and density

Using Sexstone and Fassnacht (2014) equation, the snow depth (HS, m) can be determined from the snow density as:

$$HS = \left[\frac{RHO - 844 - 1.06 \text{ DOY} - 0.004 Z + 1.78 \times 10^{-3} \text{ UTM}_e}{26.1} \right]^2 \quad (11)$$

Where, DOY = day of year (Julian day); Z = elevation, m; UTM_e = Universal Transverse Meridian Easting, which can be determined from the following set of equations:

$$\text{UTM}_e = k_4 p + k_5 p^3 \quad (12)$$

$$p = (\text{longitude}_{\text{degree}} - \text{LZCM}) \left(\frac{\pi}{180} \right) \quad (13)$$

$$\text{LZCM} = 6 \text{ LZ} - 183 \quad (14)$$

$$\text{LZ} = 31 + \text{int} \left(\frac{\text{longitude}_{\text{degree}}}{6} \right) \quad (15)$$

$$k_4 = k_0 \text{ nu} \cos(\text{latitude}_{\text{radian}}) \quad (16)$$

$$\begin{aligned} k_5 = & \left[k_0 \text{ nu} \frac{\cos^3(\text{latitude}_{\text{radian}})}{6} \right] \\ & \left[1 - \tan^2(\text{latitude}_{\text{radian}}) \right. \\ & \left. + e'^2 \cos^2(\text{latitude}_{\text{radian}}) \right] \quad (17) \end{aligned}$$

$$\text{nu} = \frac{a}{(1 - (e \sin(\text{latitude}_{\text{radian}}))^2)^{0.5}} \quad (18)$$

$$\text{latitude}_{\text{radian}} = \text{latitude}_{\text{degree}} \left(\frac{\pi}{180} \right) \quad (19)$$

where, LZCM = longitude zone central meridian, degree; LZ = longitude zone, degree; k₀ (scale factor) = 0.9996; e'² = 0.006739497; a (equatorial radius, m) = 6378137 m; e

$$(\text{eccentricity}) = \sqrt{1 - \left(\frac{b}{a} \right)^2} = 0.08181919;$$

$$b \text{ (polar radius, m)} = 6356752.314 \text{ m.}$$

The longitude degree and latitude degree are the site longitude and site latitude expressed in degree decimal format determined as:

$$\text{degree} + \left(\frac{\text{minute}}{60} \right) + \left(\frac{\text{second}}{3600} \right) \quad (20)$$

where, degree = degree, minute = minute (0–59), second = second (0–59) corresponding to site coordinates.

Using the snow depth and snow density, the SWE at pixel level can be determined using the equation given by (Bavera and de Michele, 2009):

$$SWE = HS \left(\frac{RHO}{\rho_{WATER}} \right) \quad (21)$$

where, ρ_{WATER} = density of water in kg m^{-3}
and SWE is in m.

2.6. Raster processing

The above mentioned equations were automated in an image processing software using model builder for determining snow density, snow depth and SWE layers. As shown earlier, several steps are involved in determining the RHO (Eqs. 2 through 10) (Fig. 3). In the developed RHO model, required pre-processing of the albedo images was done since the model needed the albedo values in fraction after removing the non-snow pixels. As shown in Eq. 1, in order to find out the value of RHO, Albedo (A), days since cessation of storm (D), the value of ZCOS and solar declination (SD) of the area were also needed and incorporated in the model.

For determining the snow depth (HS), another model was developed (Fig. 4). Estimation of HS (Eq. 11), involved different parameters like Z, DOY, UTMe and RHO. The developed model included various steps to calculate UTMe as mentioned in Eqs. 12 through 20.

For determination of SWE, another model was developed to execute Eq. 21, where both the previously determined snow density and snow depth are used. Pixel levels SWE values were used in generating the SWE maps for the watershed. In order to generate the average SWE of a particular month, the average of maximum, minimum and mean of all the days of the month were determined. SWE maps were generated for dominating snow months January–May 2013.

2.7. Determination of Snow Covered Area (SCA)

Snow covered area (SCA) can be referred to as the areal extent of snow-covered ground which is usually expressed as percentage of total area of the watershed. SCA (%) from the daily MODIS snow cover images was calculated by finding total number of pixels in the watershed with snow (pixel value = 200). Similarly, cloud covered area (CCA) percentages for daily images were calculated from total number of pixels with cloud (pixel value = 50).

$$SCA (\%) = \frac{\text{Total no. of Snow pixel}}{\text{Total no. of pixel}} * 100 \quad (22)$$

$$CCA (\%) = \frac{\text{Total no. of Cloud pixel}}{\text{Total no. of pixel}} * 100 \quad (23)$$

The images having CCA (%) > 5 were not considered in this study. Only images that were cloud free with CCA (%) < 5 were used for analysis. From daily SCA (%) value of the watershed for cloud free dates, average values for each month were calculated and these average SCA% values were plotted against respective months to generate snow accumulation and depletion pattern of the watershed during January–May 2013.

2.8. Validation of SWE

For validating the SWE determined by the above approach, a day-to-day comparison was carried out with Global Land Data Assimilation System (GLDAS) SWE data (Fang et al. 2008). In the absolute absence of ground measurements, this was the only possible attempt at validation. GLDAS is an LDAS (Land Data Assimilation) project with a goal of using satellite and ground observational data products along with advanced land surface modelling and data assimilation techniques for generating land surface states and fluxes (Rodell et al., 2004). GLDAS runs several land surface models, integrates a large amount of observed data, and simulates at a global scale at high resolutions (2.5° to 1 km). GLDAS drives four land surface models (LSMs): Mosaic, National Centers for Environmental Prediction/ Oregon State University/ Air Force/ Hydrologic Research Lab (NOAH) model, the

Community Land Model (CLM), and the Variable Infiltration Capacity (VIC) model. GLDAS data can be accessed via the Goddard Earth Sciences' (GES) Data and Information Services Center (DISC) (<http://disc.gsfc.nasa.gov/hydrology>) which hosts 3-hourly and monthly temporal resolution at both 1.0° and 0.25° spatial resolution archive in GRIB

format. For the present study, the 0.25° resolution, 3 hourly SWE data of NOAA LSM were downloaded from http://disc.sci.gsfc.nasa.gov/hydrology/data-holdings/parameters/snow_water_equivalent.shtml (Livneh et al., 2010).

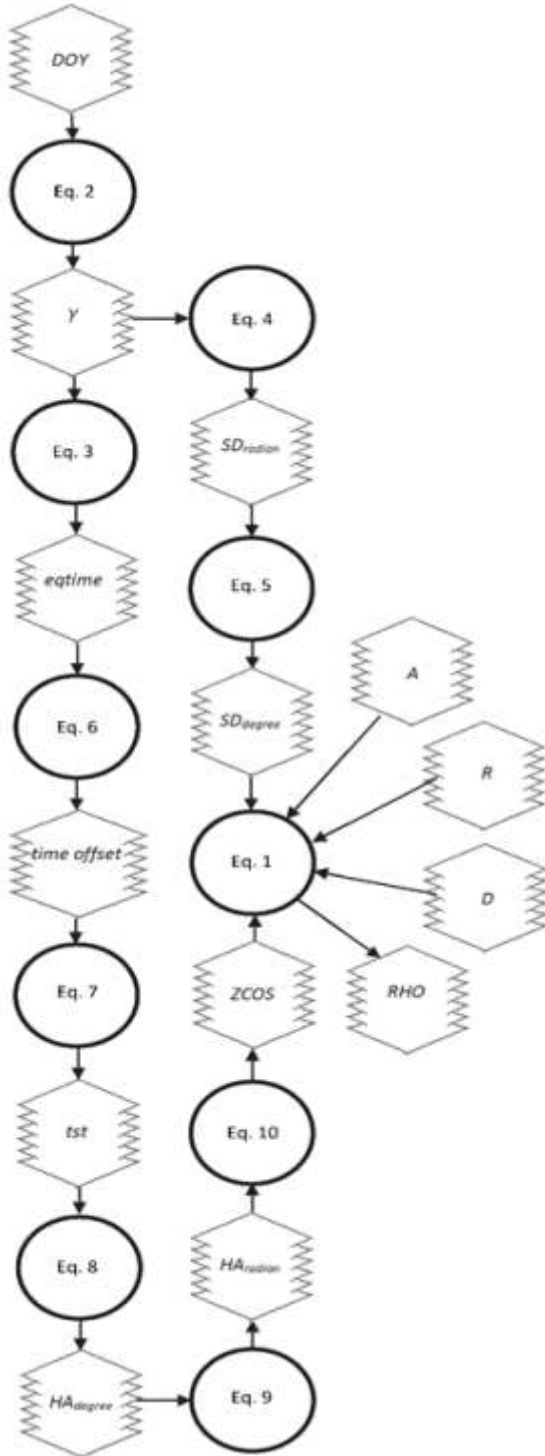


Fig. 3. Developed RHO model.

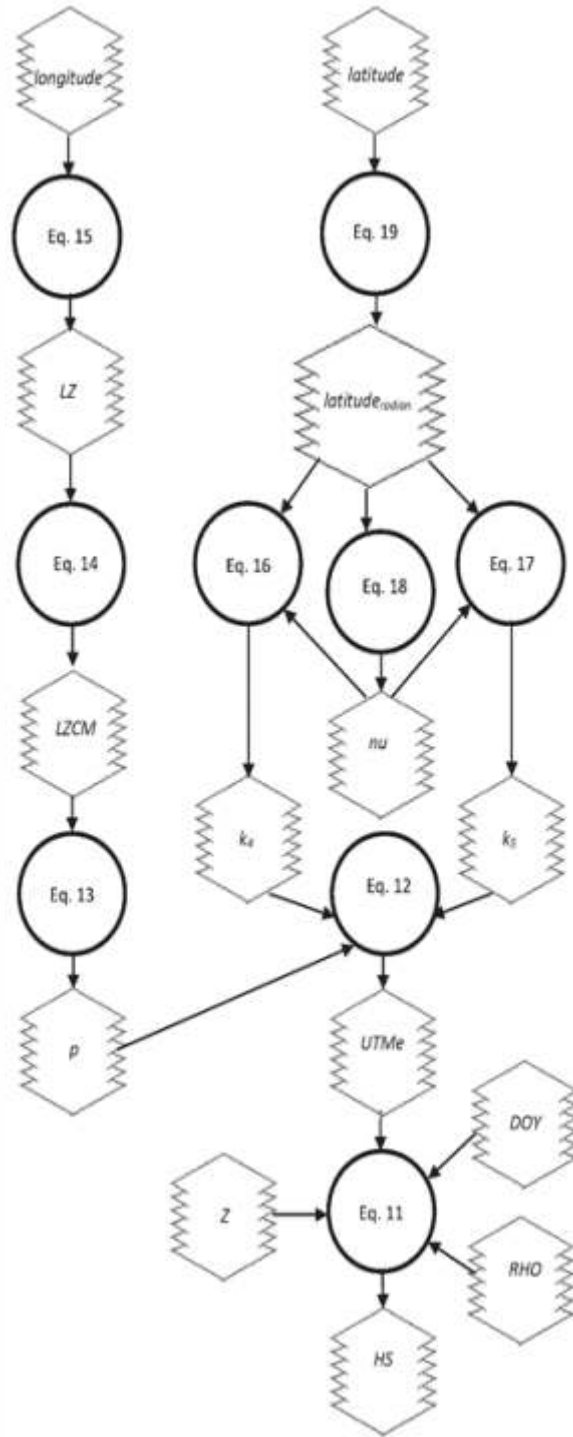


Fig. 4. Developed HS model.

3. Results and discussion

3.1. Accuracy assessment of MODIS Albedo

Monthly comparison results between MODIS and AWS-measured albedo for snow year 2012-13 are presented in Fig. 5. Comparison could be performed for November 2012, and February–March 2013 only, as the AWS pixel was under cloud cover in other months. The comparison results found the MODIS albedo product to be sufficiently accurate. Further details of these comparisons are available in Bandyopadhyay et al. (2016).

3.2. Determination of Snow Density, Snow Depth and SWE

The snow density for the dominating snow months (Jan–May) of the year 2012–2013 were determined. There were some days with considerable cloud cover and also a few days with missing data which acted as a hindrance to get daily snow albedo. Due to some missing data, instead of daily, the monthly variation of snow density for the study area was determined. This was done by taking the average of the maximum, minimum and mean of snow density for the available days in a particular month when number of snow covered pixels were significant. The monthly snow density variation has also been plotted in Fig. 6(a). It shows an increase of snow density from January to May. The mean of the snow density was lowest in January, 2013 with 343.36 kg m⁻³ and highest in the month of May with 417.38 kg m⁻³. Fresh snow has lesser density and it increases with time. Snow density is more when

snow becomes ripened.

In the same way as snow density, the average of the daily maximum, minimum and mean snow depths were determined for the available days in a particular month when number of snow covered pixels were significant. The monthly snow depth variation has been plotted in Fig. 6(b). An increase in snow depth value was found from January to February and then it decreased till May. The curve shows a peak in the month of February where the average maximum value of snow depth was as high as 3.045 m and in the month of May, average maximum snow depth was found as low as 1.640 m.

Finally, SWE of the dominating snow months of year 2012–2013 was determined from snow density and snow depth. The average of the daily maximum, minimum and mean of the snow water equivalents were carried out in the same way as it was done in case of RHO and snow depth. The monthly variation of the SWE of the study area is shown in Fig. 6(c), where, a peak is found in the month of February. From the Fig. 6(c), the highest SWE was found in the month of February 2013 against the lowest in the month of May 2013. The average maximum SWE is 1.051 m whereas average minimum value is about 0.003 m. SWE was found to be more sensitive to HS compared to RHO. At constant RHO, SWE and HS are directly related and SWE followed the same trend as HS. Even if RHO increased, SWE decreased with decreasing HS and vice versa (Fig. 7).

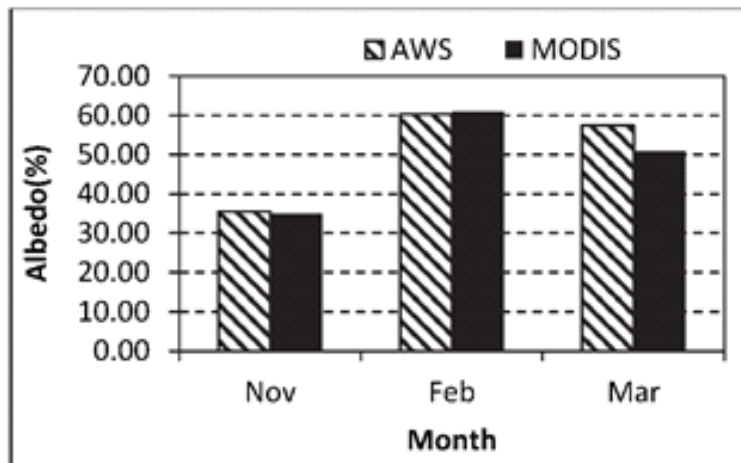


Fig. 5. Comparison of MODIS snow albedo and AWS recorded albedo.

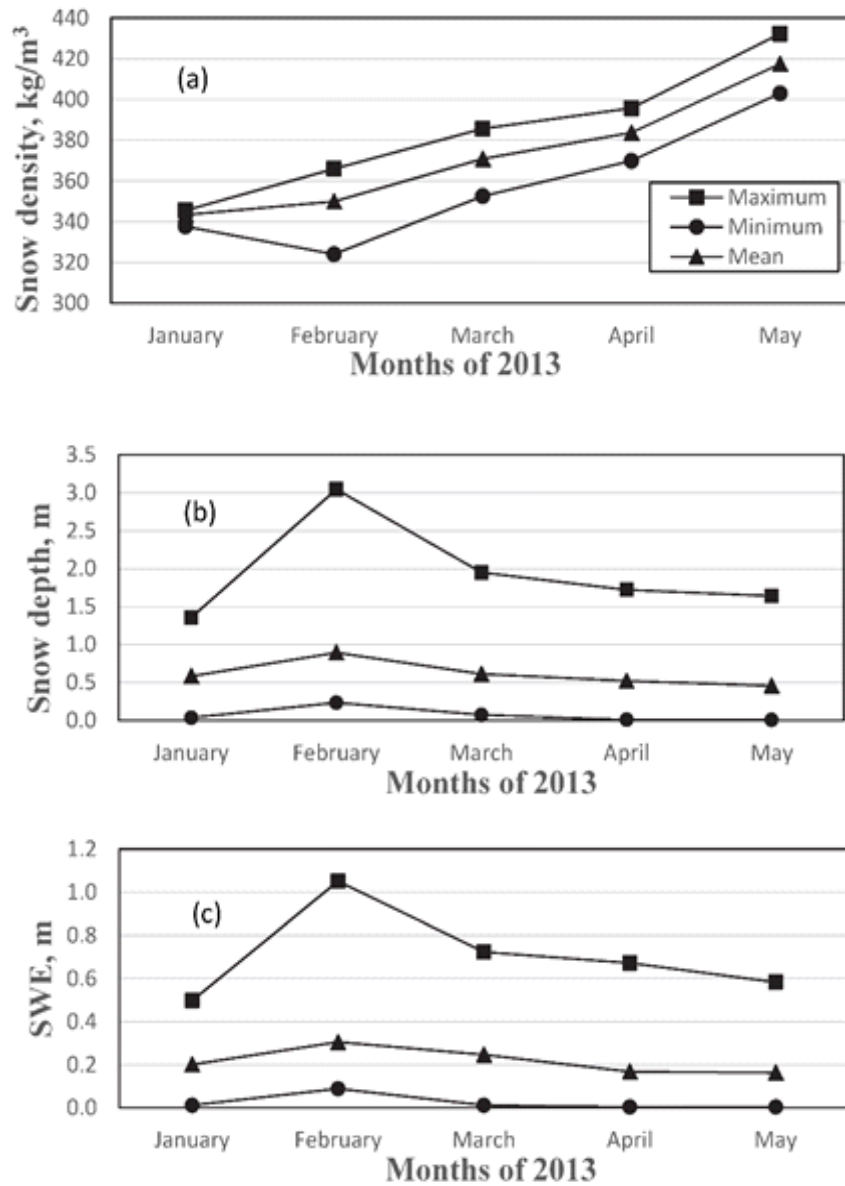


Fig. 6. Monthly variation of (a) snow density, (b) snow depth and (c) SWE.

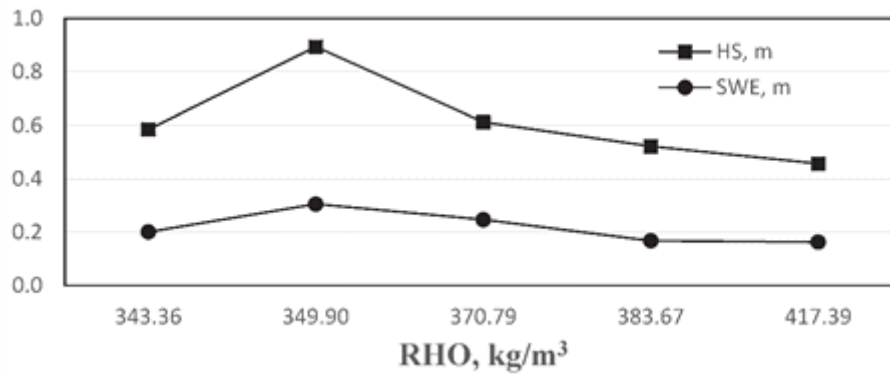


Fig. 7. Relationship between RHO, HS and SWE.

3.3 Validation of SWE

For the cloud-free days of the dominating snow months (Jan–May) of 2013, for which there were no missing albedo data pixels, the above determined SWE values were compared with the 0.25° resolution, 3 hourly SWE data of NOAH LSM downloaded from GLDAS. The entire Nuranang catchment was contained within a single $0.25^\circ \times 0.25^\circ$ pixel and hence, the determined SWE values were averaged over space (snow pixels only) whereas the NOAH LSM 3 hourly SWE values were averaged over time (24 hours). The comparison plot is shown in Fig. 8. It can be seen that the lower SWE values are a bit scattered in the 1:1 comparison plot, whereas, the higher SWE values are generally slightly over estimated by the present study. Although, overall the performance of the present approach can be considered as usable.

3.4. Generation of representative monthly maps

The snow density, snow depth and SWE maps were generated for dominating snow months (Jan–May) of year 2012–2013. Because of the aberration in the data due to cloud cover and missing pixels, it was difficult to show the daily variability of all three parameters. Hence, a day in each month was chosen in such a way that it has the highest

number of snow pixels compared to other cloud free days in that month to represent that particular month. Therefore, five days, one from each month, were selected and the snow density, snow depth and SWE maps were generated as shown in Figs. 9 through 11. From the snow density maps, it can be seen that 11th January has the lowest value ranging from 307.12 kg m⁻³ to 328.19 kg m⁻³ considering all snow pixels whereas it increases till the month of May with maximum value of 422.30 kg m⁻³ on 3rd May.

It can be observed from the maps that, the number of snow pixels are less in the month of January and increases till February. Then gradually it decreases till May. From the generated snow depth maps (Fig. 10), it is found that the snow depth increases from the month of January up to February, where it has its highest value ranging from 0.001 m to 4.846 m considering all snow pixels on 19th February, and then decreases till May. The high ranges in the snow depth values may be both due to the variation in elevation of the study area and their seasonal variability. The generated SWE maps are shown in Fig. 11. SWE values also increase from January to February and then decrease till May. Considering all snow pixels in the watershed, highest SWE was obtained on 19th February with maximum value of 1.417 m and lowest on 3rd May as 0.822 m.

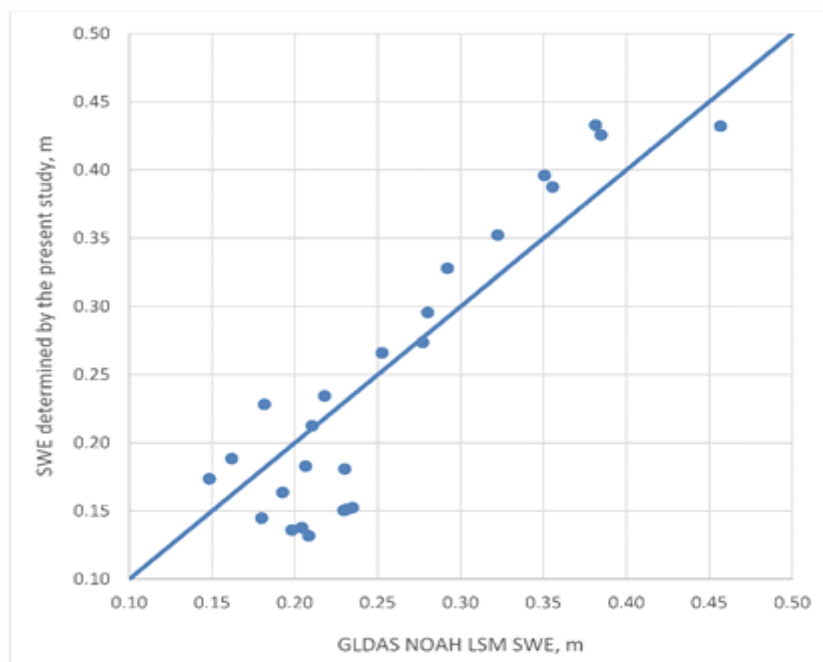


Fig. 8. Comparison of estimated SWE with GLDAS NOAH LSM simulated SWE.

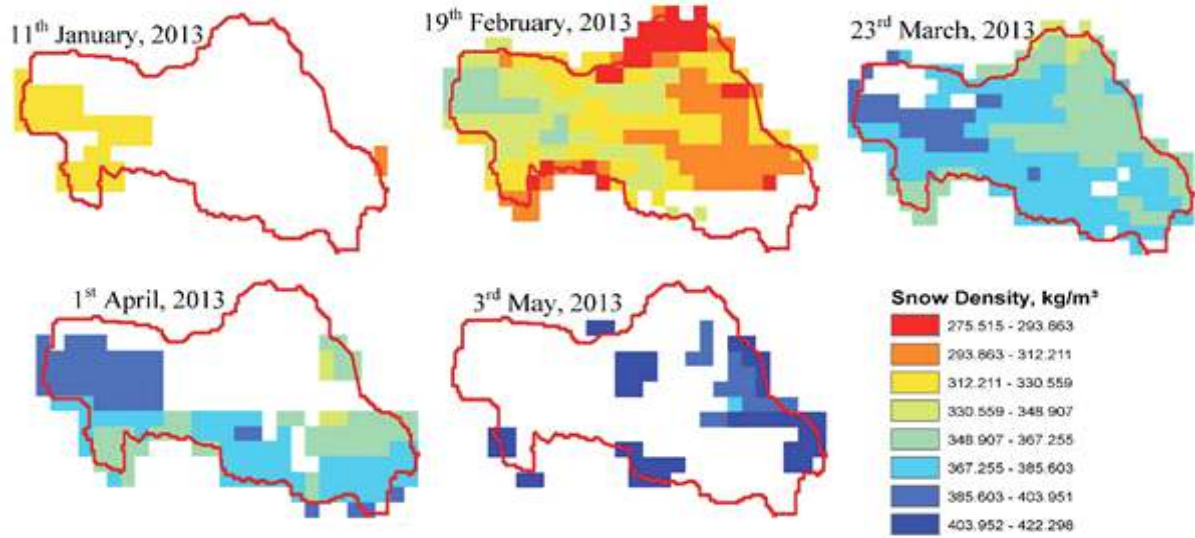


Fig. 9. Snow density maps.

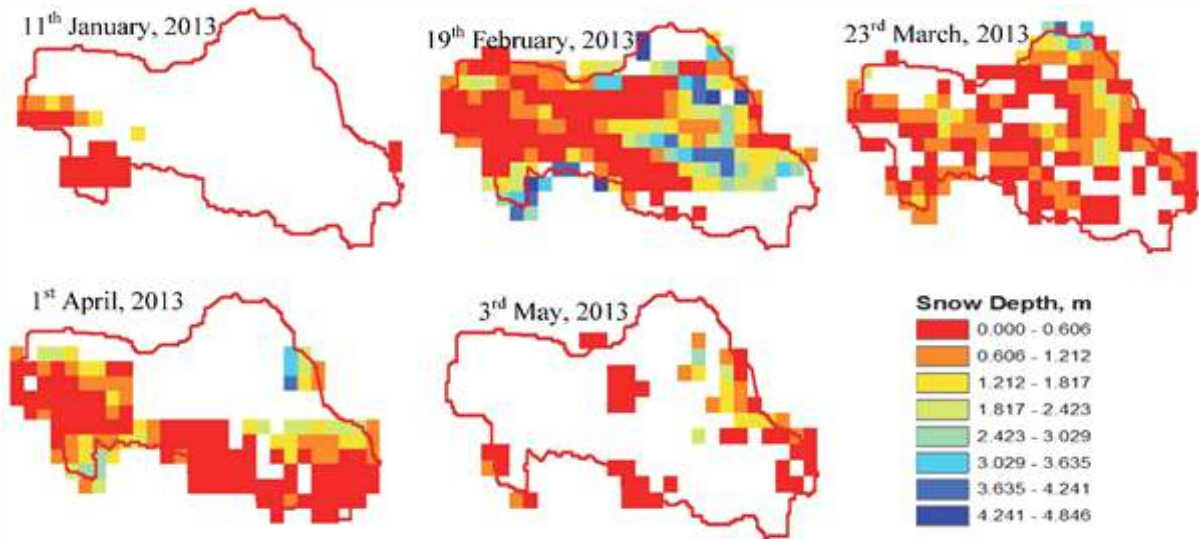


Fig. 10. Snow depth maps.

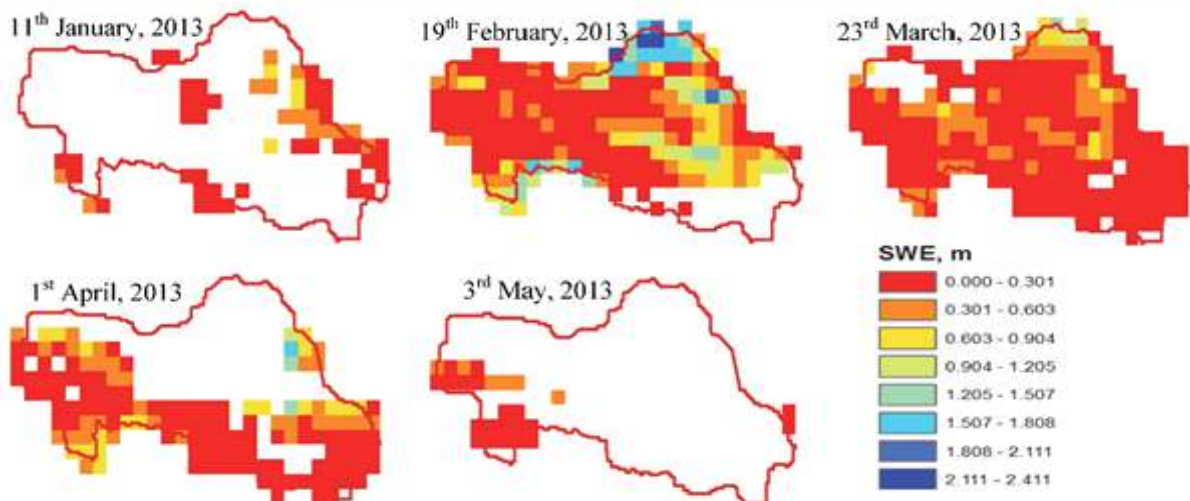


Fig. 11. Snow water equivalent maps.

3.5. Monthly variation of SCA

The average of the daily SCA (%) was obtained for the cloud free days in a particular month. From Table 1, it can be inferred that January has the least SCA with an average of only 0.55 sq. km while the month of February has the highest SCA with an average of 16.8 sq. km. The plot of SCA (%) against the corresponding month of 2013 is shown in figure 12. It can be seen that the SCA% in February is the highest with 32.31% and decreases gradually to 2.38% in the month of May.

3.6. Inter-relationship among RHO, HS, SWE, SCA and Mean Monthly Temperature.

The monthly representative values of RHO, HS, SWE, and SCA (%) along with the mean monthly temperature are plotted in figure 13. The monthly variation of HS, SWE and SCA (%) are seen to follow the same trend with a peak in the month of February 2013. The RHO plot shows different trend compared to other three. It increases gradually from the month of January to May. figure 13 shows that rise in temperature have a positive relationship with RHO while a negative relation with HS, SWE and SCA (%). Both RHO and temperature increase with time starting from February, which has the minimum temperature, and it gradually increases up to May. Temperature

corresponds negatively with HS, SWE and SCA (%) as all of these are having their peak in the month of February with decreasing trend till May.

3.7. Comparison to other studies

It is important to compare these results with other studies carried out in similar topography to check their accuracy. The present study reveals the value of RHO of the study area ranging between 340–420 kg m⁻³. These are in similar ranges with the findings of Singh et al. (2011) where RHO ranges from 280 to 440 kg m⁻³ in Himalayan region. on the other hand, the estimated SWE in the present study area have been found to be generally ranging from 0.16 to 0.3 m with very few pixels having higher than 1.0 m extending maximum up to 2.0 m. These values of SWE are also found to be matching with values reported by other researchers (0.2 m to 1.5 m by Menegoz et al., 2013). The spatial distribution of SWE also showed a higher SWE value with higher elevation which corresponds to the conclusion made by Stigter et al. (2017). HS determined in the present study ranges mostly between 0.4 and 0.9 m with only few pixels having values greater than 3.0 m and extending maximum up to 4.8 m. These are found to have similarity with the findings of other researchers where the HS extended up to 3.19 m (Kumar et al., 2006; Datt et al., 2008).

Table 1. Average Monthly SCA of Nuranang basin, 2013

Year 2013	Snow cover area (SCA)	
Month	SCA, sq. km	SCA, %
January	0.55	1.06
February	16.80	32.31
March	11.50	22.11
April	2.70	5.18
May	1.24	2.38

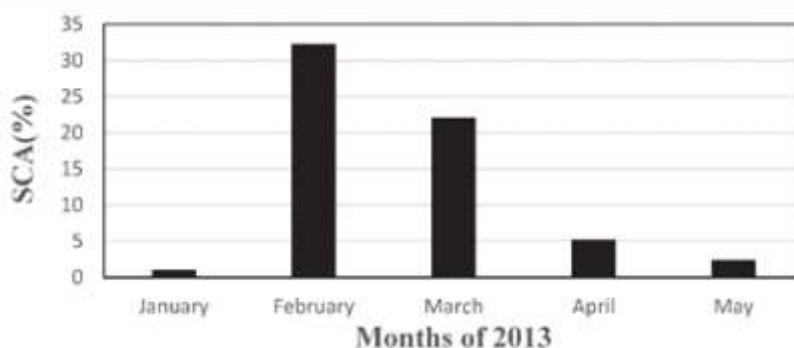


Fig. 12. Monthly variation of SCA.

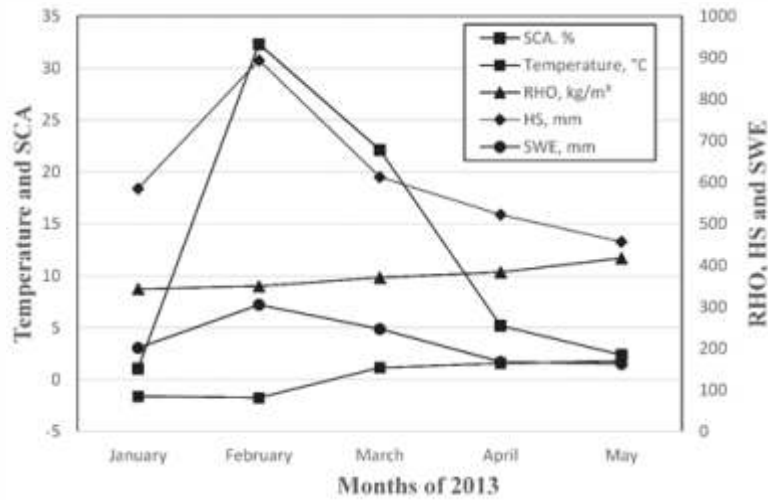


Fig. 13. Inter-comparison among RHO, HS, SWE, SCA and mean monthly temperature.

4. Conclusions

The study deals with the determination of the snow density (RHO), snow depth (HS) and SWE using remotely sensed satellite images and assessing the usability of determined SWE. The value of RHO under present study was found to be in the ranges of 340–420 kg m⁻³. An increase in RHO was seen from January to May. HS determined in the present study ranges mostly between 0.4 and 0.9 m whereas SWE, on the other hand, generally ranges from 0.16 to 0.3 m. The temporal distribution of both HS and SWE showed February obtaining the highest value during the study period. The spatial distribution of SWE over the study area also showed a considerably higher SWE in areas with higher elevation. Temperature corresponds negatively with HS, SWE and SCA (%) with their peak in the month of February and decreasing till May. By comparing the results of the present study with other published data collected from relevant research works on the Himalayan river basin and with SWE data generated by LSM simulations, it can be said that one can estimate reasonable snow density, snow depth and SWE values for their respective non-instrumented and inaccessible mountainous study area by using satellite images of snow albedo, temperature, precipitation and the DEM as input to the models developed in this study. However, the accuracy of the results needs to be further assessed on spatial and temporal scale against observed data, which could not be done in the present study for non-availability of measured data.

Acknowledgements

The authors duly acknowledge the NASA Distributed Active Archive Centre (DAAC) and the National Snow and Ice Data Centre (NSIDC) for making the MODIS snow albedo, MODIS LST, and SRTM DEM data freely available for download; along with the Goddard Earth Sciences' (GES) Data and Information Services Center (DISC) and National Centers for Environmental Prediction/ Oregon State University/ Air Force/ Hydrologic Research Lab (NOAH) for making the Global Land Data Assimilation System (GLDAS) SWE data freely available for download. The authors also thank the University Grants Commission, Govt. of India for the “Post-Graduate Scholarship for Professional Courses for SC/ST Candidates” received by Ms. G. Nengzouzam during this study undertaken as her M.Tech project.

Authors' Contribution

Grace Nengzouzam, did the actual work as part of her Master's thesis. Ngahorza Chiphang, wrote the codes for the models developed. Shelina Rajkumari, verified the results independently. Liza G Kiba, verified the approach in other watersheds of Himalayan region to make sure these methods produce results with sufficient accuracy. Arnab Bandyopadhyay, helped in code writing and debugging, ERDAS model development, and manuscript writing. Aditi Bhadra, conceptualized the work.

References

- Avanzi, F., De Michele, C., Ghezzi, A., 2015. On the performances of empirical regressions for the estimation of bulk snow density. *Geografia Fisica e Dinamica Quaternaria*, 38, 105–112.
- Bandyopadhyay, A., Mishra, P., Chiphang, N., Kumar, A., Tripathy, S., 2016. Validation of Broadband Snow Albedo Derived from AWiFS for Eastern Himalaya. 7th International Conference on Water Resources and Environment Research (ICWRER 2016), Kyoto, Japan, June 05–09, g02-02-1–6.
- Bavera, D., de Michele, C., 2009. Snow Water Equivalent estimation in Mallero basin using snow gauge data and MODIS images and fieldwork validation. *Hydrol. Processes*, 23(14), 1961–1972.
- Bavera, D., Bocchiola, D., de Michele, C., 2007. A statistical estimation of Snow Water Equivalent coupling ground data and MODIS images. AGU Fall Meeting Abstracts, <http://adsabs.harvard.edu/abs/2007AGU FM.C21B0452B>.
- Chiphang, N., Mishra, P., Bandyopadhyay, A., Bhadra, A., 2017. Temporal Variations in Snow Albedo at Glaciated Upper Elevation Zone of an Eastern Himalayan River Basin. In: Pant, N.C., Ravindra, R., Srivastava, D., Thompson, L.G. (Eds.), *Himalayan Cryosphere: Past and Present*. Geological Society, London, Special Publications, 462.
- Datt, P., Srivastava, P.K., Negi, P.S., Satyawali, P. K., 2008. Surface energy balance of seasonal snow cover for snowmelt estimation in N-W Himalaya. *Journal of Earth Syst. Sci.*, 117(5), 567–573.
- Elder, K., Rosenthal, W., Davis, R.E., 1998. Estimating the spatial distribution of snow water equivalence in a montane watershed. *Hydrol. Processes*, 12, 1793–1808.
- Fang, H., Hrubiak, P.L., Kato, H., Rodell, M., Teng, W.L., Vollmer, B.E., 2008. Global land data assimilation system (GLDAS) products from NASA hydrology data and information services centre (HDISC). ASPRS 2008 Annual Conference.
- Hall, D. K., Riggs, A.G., Salomonson, V., 1995. Development of Method for Mapping Global Snow Cover using Moderate Resolution Imaging Spectroradiometer Data. *Remote Sens. Environ.*, 54(2), 127–140.
- Hall, D. K., G. A. Riggs, V. V., Salomonson, 2006. MODIS/Terra Snow Cover 5-Min L2 Swath 500m. Version 5. Boulder, Colorado USA: NASA National Snow and Ice Data Center Distributed Active Archive Center. doi: 10.5067/actyzb9beos.
- Hassan, Q. K., Sekhon, N.S., Magai, R., McEachern, P., 2012. Reconstruction of snow water equivalent and snow depth using remote sensing data. *Journal of Environmental Informatics*, 20(2), 67–74.
- Jonas, T., Marty, C., Magnusson, J., 2009. Estimating the snow water equivalent from snow depth measurements in the Swiss Alps. *J. Hydrol.*, 378, 161–167.
- Kumar, V., Rao, Y., Venkataraman, G., Sarwade, R., Snehani., 2006. Analysis of Aqua AMSR-E Derived Snow Water Equivalent over Himalayan Snow Covered Regions. IEEE International Symposium on Geoscience and Remote Sensing, Denver, CO, 702–705.
- Livneh, B., Xia, Y., Mitchell, K.E., Ek, M.B., Lettenmaier, D. P., 2010. Noah LSM snow model diagnostics and enhancements. *J. Hydrometeorology*, 11, 721–738.
- Menegoz, M., Gallee, H., Jacobi, H.W., 2013. Precipitation and snow cover in the Himalaya: from reanalysis to regional climate simulations. *Hydrol. Earth Syst. Sci.*, 17, 3921–3936.
- Mishra, P., Zaphu, V. V., Monica, N., Bhadra, A., Bandyopadhyay, A. 2016. Accuracy assessment of MODIS fractional snow cover product for an eastern Himalayan catchment. *J. Indian Soc. Remote Sens.*, 44(6), 977–985.
- Rodell, M., Houser, P. R., Jambor, U., Gottschalck, J., Mitchell, K., Meng, C. J., Arsenault, K., Cosgrove, B., Radakovich, J., Bosilovich, M., Entin, J. K., Walker, J. P., Lohmann, D., Toll, D., 2004. The Global Land Data Assimilation System. *Bull. Am. Meteorol. Soc.*, 85(3), 381–394.
- Senzeba, K. T., Bhadra, A., Bandyopadhyay, A., 2015. Snowmelt runoff modelling in data scarce Nuranang catchment of eastern Himalayan region. *Remote Sens. Appl.: Soc. Environ.*, 1: 20-35. ISSN: 2352-39385. doi: 10.1016/j.rsase.2015.06.001.
- Sexstone, G. A., Fassnacht, S. R., 2014. What drives basin scale spatial variability of snowpack properties in northern Colorado? *The Cryosphere*, 8, 329–3344.
- Singh, K. K., Datt, P., Sharma, V., Ganju, A., Mishra, V. D., Parashar, A., Chauhan,

- R., 2011. Snow depth and snow layer interface estimation using Ground Penetrating Radar. *Current Science*, 100(10), 1532–1539.
- Smith, J.L., Halverson, H.G., 1979. Estimating snowpack density from albedo measurement. Res. Pap. PSW-RP-136. Berkeley, CA: U.S. Department of Agriculture, Forest Service, Pacific Southwest Forest and Range Experiment Station. 13.
- Stigter, E.E., Wanders, N., Saloranta, T.M., Shea, J.M., Bierkens, M.F.P., Immerzeel, W.W. 2017. Assimilation of snow cover and snow depth into a snow model to estimate snow water equivalent and snowmelt runoff in a Himalayan catchment. *The Cryosphere*, 11, 1647-1664.
- Takala, M., Luojus, K., Pulliainen, J., Derksen, C., Lemmetyinen, J., Kärnä, J-P., Koskinen, J., Bojkov, B., 2011. Estimating northern hemisphere snow water equivalent for climate research through assimilation of space-borne radiometer data and ground-based measurements, *Remote Sens. Environ.*, 115(12), 3517–3529.